This is the **peer reviewed version** of the following article: Ganesamoorthy, C.; Krüger, J.; Wölper, C.; Nizovtsev, A.S.; Schulz, S.: Reduction of [Cp*Sb]4 with Subvalent Main‐Group Metal Reductants: Syntheses and Structures of [(L1Mg)4(Sb4)] and [(L2Ga)2(Sb4)] Containing Edge‐Missing Sb4 Units. *Chemistry - A European Journal*, 2017, 23, 2461-2468, which has been published in final form at: https://doi.org/10.1002/chem.201605547

Reduction of $[Cp^*Sb]_4$ with subvalent main group metal reductants - syntheses and structures of $[(L^1Mg)_4(Sb_4)]$ and $[(L^2Ga)_2(Sb_4)]$ containing edge-missing Sb_4 units

Chelladurai Ganesamoorthy,[a] Julia Krüger,[a] Christoph Wölper,[a] Anton S. Nizovtsev,[b,c] and Stephan Schulz[a]*

Abstract: $[Cp^*Sb]_4$ ($Cp^* = C_5Me_5$) reacts with $[L^1Mg]_2$ and L^2Ga with formation of $[(L^1Mg)_4(\mu_4,\eta^{1:2:2:2}\text{-}Sb_4)]$ {L^1 = *i*-$Pr_2NC[N(2,6\text{-}i\text{-}Pr_2C_6H_3)]_2$, **1**} and $[(L^2Ga)_2(\mu,\eta^{2:2}\text{-}Sb_4)]$ {L^2 = $HC[C(Me)N(2,6\text{-}i\text{-}Pr_2C_6H_3)]_2$, **2**}. The cleavage of the Sb-Sb and Sb-C bonds in $[Cp^*Sb]_4$ are the crucial steps in both reactions. The formation of **1** occurred *via* elimination of the Cp* anion and formation of Cp^*MgL^1, while **2** was formed by reductive elimination of Cp^*_2 and oxidative addition of L^2Ga to the Sb_4 unit. **1** and **2** were characterized by heteronuclear NMR spectroscopy and single crystal X-ray diffraction and their bonding situation was studied by quantum chemical calculations.

Introduction

Salt-like Zintl ions A_xE_y ($x \leq y$) consisting of p-block polyanions (E_y^{n-}) and s-block cations (A_x^{m+}) have been intensively studied since their first discovery in the early 1900.[1] They were initially prepared by reactions of the bulk metals and intermetallic alloys with Na in liquid NH_3, while more stable solutions were formed in polar aprotic solvents, i.e. ethylenediamine, dimethylformamide, or by use of cryptands, i.e. [2,2,2]crypt, [18]crown-6. Many Zintl ions have been prepared from the elements in typical solid state reaction, but bottom-up strategies using molecular precursors also allowed the synthesis of discrete atom clusters by reduction or reductive elimination reactions.[2] For example, thermolysis of $\{[Sb(PCy)_3]_2Li_6\cdot 6HNMe_2\}$ in toluene at 40 °C gave the Zintl compound $[Sb_7Li_3\cdot 6HNMe_2]$ *via* reductive elimination of $(CyP)_4$,[2a] while ligand-stabilized polyanions were obtained by activation reactions of white phosphorus P_4 and yellow arsenic As_4 with organometallic compounds. The resulting complexes include Sc- and Sm-substituted realgar-type P_8 polyphosphides $[(L_2M)_4(P_8)]$ (L = Cp*, 1,1'-fc(NSi^tBuMe_2)$_2$),[3] transition metal-coordinated $E_{4\text{-}8}$ cages, i.e. $[\{Cp^{big}Fe(CO)_2\}_2(\mu,\eta^{1:1}\text{-cage})]$ (Cp^{big} = $C_5(4\text{-}n\text{-}BuC_6H_4)_5$; cage = P_4, As_4, P_4S_3, P_4Se_3),[4] $[\{Cp'Fe(CO)_2\}_2((\mu,\eta^{1:1}\text{-}E_4)]$ (Cp' = 1,2,4-*t*-$Bu_3C_5H_2$), $[\{Cp^*Cr(CO)_3\}_2((\mu,\eta^{1:1}\text{-}E_4)]$ (E = P, As), $\{[Cp^*IrCO]_2P_8[Cr(CO)_5]_3\}$,[5] as well as Lewis acid- and base-stabilized P_4 and P_8 clusters such as $[(L^2Mg)_2(n\text{-}Bu)_2P_4]$, $[(L^2Mg)_2(n\text{-}Bu)_2P_8]$,[6] $[(Ar)P_4(LiB(C_6F_5)_3)]$ (Ar = 2,6-dimesitylphenyl, 2,4,6-*t*-$Bu_3C_6H_2$)[7] and $[P_8\{Si(SiMe_3)_3\}_2\cdot K([18]crown\text{-}6)]$, respectively.[8] In addition, neutral E_4 (E = P, As) tetrahedra have recently been shown to be stable in the coordination sphere of different transition metals such as Cu^I, Ag^I, Au^I and Ru^{II}.[9]

Burford and Weigand et. al. developed a versatile reductive catenation reaction for the synthesis of group 15 polycations using phosphine (or arsine) as ligand and reductant.[10] For instance, reductive elimination of fluorophosphonium cations from $[(Ph_3P)_2SbF(OTf)_2]$ or from the mixture of PR_3 (R = Me, Et, Pr, Bu or Ph) and Sb^{III} salts {$FSb(OTf)_2$ or $Sb(OTf)_3$} yielded cations such as $[(R_3P)_4Sb_4](OTf)_4$ and $[(Ph_3P)_4Sb_6](OTf)_4$.[10b-d] Similarly, the dication $[(Ph_3As)_2P_4]^{2+}$ and trication $[(Ph_3As)_3P_7]^{3+}$ were obtained from one-pot reduction reactions of PCl_3 with Ph_3As or $Ph_3As(OTf)_2$ in the presence of $AlCl_3$.[10e,f] We recently showed that the reaction of $Sb(NMe_2)_3$ with L^2Ga yielded the distibene $L^2Ga(Me_2N)Sb{=}SbGa(Me_2N)L^2$, which upon heating gave $[\{L^2(Me_2N)Ga\}_2Sb_4]$, the first Sb analogue of bicyclo[1,1,0]butane formally containing a $[Sb_4]^{2-}$ dianion.[11] In addition, the reaction of distibines R_4Sb_2 (R = Me, Et) containing divalent Sb atoms with $[L^{2,3}Mg]_2$ yielded the Zintl-type ions $[(L^{2,3}Mg)_4(\mu_4,\eta^{2:2:2:2}\text{-}Sb_8)]$ {L^3 = $HC[C(Me)N(2,4,6\text{-}Me_3C_6H_2)]_2$},[12] while the analogous reaction with L^2M (M = Al, Ga) proceeded with insertion of L^2M into the Sb-Sb bond and subsequent formation of $L^2M(SbEt_2)_2$.[13] We now focused on reduction reactions of *cyclo*-tetrastibine $[Cp^*Sb]_4$, which formally contains monovalent Sb atoms, and report herein on the synthesis of $[(L^1Mg)_4(\mu_4,\eta^{1:2:2:2}\text{-}Sb_4)]$ **1** (L^1 = *i*-$Pr_2NC[N(2,6\text{-}i\text{-}Pr_2C_6H_3)]_2$) and $[(L^2Ga)_2(\mu,\eta^{2:2}\text{-}Sb_4)]$ **2** (L^2 = $HC[C(Me)N(2,6\text{-}i\text{-}Pr_2C_6H_3)]_2$). **1** and **2** both have formally tetraanionic $[Sb_4]^{4-}$ polyanions as central structural motif, but both their connectivity as well as bonding nature clearly differs.

Results and Discussion

$[Cp^*Sb]_4$ reacts at room temperature with $[L^1Mg]_2$ with elimination of L^1MgCp^* and formation of $[(L^1Mg)_4(\mu_4,\eta^{1:2:2:2}\text{-}Sb_4)]$ **1**, whereas the reaction with L^2Ga proceeded only at higher reaction temperature (71 °C) with elimination of Cp^*_2 and formation of $[(L^2Ga)_2(\mu,\eta^{2:2}\text{-}Sb_4)]$ **2**. The molar ratio for both reactions were optimized *via in situ* ^1H NMR experiments by varying the concentration of $[L^1Mg]_2$ and L^2Ga versus $[Cp^*Sb]_4$. The ^1H NMR spectra of 4:1 (for **1**) and 2:1 (for **2**) molar ratio reaction mixtures

[a] Dr. C. Ganesamoorthy, B. Sc. J. Krüger, Dr. C. Wölper, Prof. Dr. S. Schulz
Faculty of Chemistry and Center for NanoIntegration (CENIDE), University of Duisburg-Essen
Universitätsstr. 5-7, S07 S03 C30, D-45117 Essen
Fax: (+) 201-183 3830; E-mail: stephan.schulz@uni-due.de
https://www.uni-due.de/ak_schulz/index_en.php
[b] Dr. A. S. Nizovtsev
Nikolaev Institute of Inorganic Chemistry, Siberian Branch of the Russian Academy of Sciences, Academician Lavrentiev Avenue 3, 630090, Novosibirsk, Russian Federation
[c] Novosibirsk State University, Pirogova Street 2, 630090, Novosibirsk, Russian Federation

Supporting information for this article (experimental details including ^1H, ^{13}C NMR, IR spectra and computational details) is available on the WWW under http://dx.doi.org/xxx</.

Accepted Manuscript. *This article may be used for non-commercial purposes in accordance with Wiley Terms and Conditions for Use of Self-Archived Versions.*

almost exclusively showed the formation of **1** and **2** together with the elimination products L^1MgCp^* and decamethyl-1,1'-dihydrofulvalene Cp^*_2 (Fig. S5, Fig. S11). Addition of an excess of $[L^1Mg]_2$ or L^2Ga also only yielded **1** and **2**. The key steps in both reactions are the cleavage of the Sb-C bonds, which occurred either by heterolytic bond breakage and formation of the Cp* monoanion, which then reacts with formation of L^1MgCp^*, or by homolytic bond breakage and formation of Cp^*_2.

1 dissolved partially in benzene and toluene but was insoluble in hexane and pentane. In contrast, **2** dissolved well in benzene and toluene, while its partial solubility in hexane allowed the isolation of pure **2** by slowly cooling a warm hexane solution to 8 °C. **1** and **2** are unstable toward air and moisture but can be stored at room temperature for months under argon. **1** is thermally stable in a solution of toluene-d_8 up to 120 °C, while **2** was found to readily decompose into L^2Ga and elemental Sb under these conditions (Fig. S10, Fig. S14).

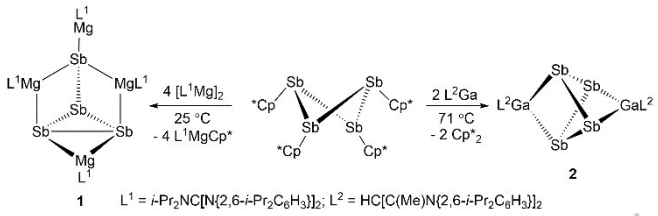

Scheme 1. Synthesis of **1** and **2**.

The ^{1}H NMR spectrum of **1** in toluene-d_8 showed characteristic resonances of the L^1 ligand. The ^{13}C NMR spectrum of **1** showed totally 17 signals, which were addressed to 10 isopropyl, one N_3C (167.6 ppm) and 6 aromatic carbon atoms. Although ^{1}H NMR signals split into several broad multiplets at -80 °C, a distinct multiplicity for all four chemically inequivalent L^1 ligand was not observed. Temperature-dependent ^{1}H NMR spectra in the temperature range from 40 to 100 °C showed no specific change of the spectral pattern (Fig. S4). ^{1}H and ^{13}C NMR spectra of **2** in C_6D_6 showed a C_{2V} symmetric spectral pattern similar to that of L^2Ga and L^2Ga-M(C_6F_5)$_3$ (M = B, Al, Ga).[14] The ^{1}H NMR spectrum of **2** showed two doublets at 1.10 and 1.54 ppm and one septet at 3.72 ppm for the isopropyl groups as well as two singlets for the γ-C*H* (4.75 ppm) and phenyl groups (7.11 ppm). The ^{13}C NMR spectrum shows 11 signals, which are consistent with the C_{2V} symmetric β–diketiminate group.

The molecular structures of **1** and **2** were determined by single crystal X-ray diffraction. Single crystals of **1** and **2** were obtained from saturated benzene and hexane solutions, respectively. **1** crystallizes in the monoclinic space group $P2_1$ and **2** in the orthorhombic space group $P2_12_12_1$.[15] The core structure of **1** shows a Mg_4Sb_4 moiety, in which the Sb_4^{4-} unit is substituted by a terminal and three bridging L^1Mg^+ fragments. The Sb atoms within the Sb_4^{4-} unit adopt different formal oxidation states since Sb1 is only bonded to three Sb atoms, while Sb3 and Sb4 are each coordinated to two Sb and two Mg atoms. In contrast, Sb2 only binds to one Sb atom but three Mg atoms. The Mg atoms are threefold- (Mg1) and fourfold-coordinated (Mg2, Mg3, Mg4).

Despite the presence of different coordination modes, the Mg-N bond distances (2.009(4)-2.066(4) Å) and N-Mg-N bite angles (65.25(15)-67.10(17)°) of the L^1Mg^+ units do not differ very much and are comparable to those reported for $[L^1Mg]_2$ (Mg1-N1 2.0736(10) Å, N1-Mg1-N1 65.54(5)°) and $[L^1Mg(\mu\text{-}I)_2Mg(OEt_2)L^1]$ (*av.* Mg-N 2.066 Å, N1-Mg1-N2 66.47(8), N4-Mg2-N5 64.33(8)°).[16] The Mg1-Sb2 distance (2.7019(17) Å) is slightly shorter than the Mg4-Sb3 (2.7600(17) Å) and Mg4-Sb4 distances (2.7576 (16) Å), whereas the Mg3-Sb2 (2.8444(16) Å) and Mg3-Sb4 distances (2.7999(16) Å) are significantly elongated. It should be noted that the Mg1-Sb2 bond distance (2.7019(17) Å) is shorter than the sum of the covalent radii (Mg = 1.39 Å; Sb = 1.40 Å),[17] but considering the disorder of Sb-core, these values should not be overrated.

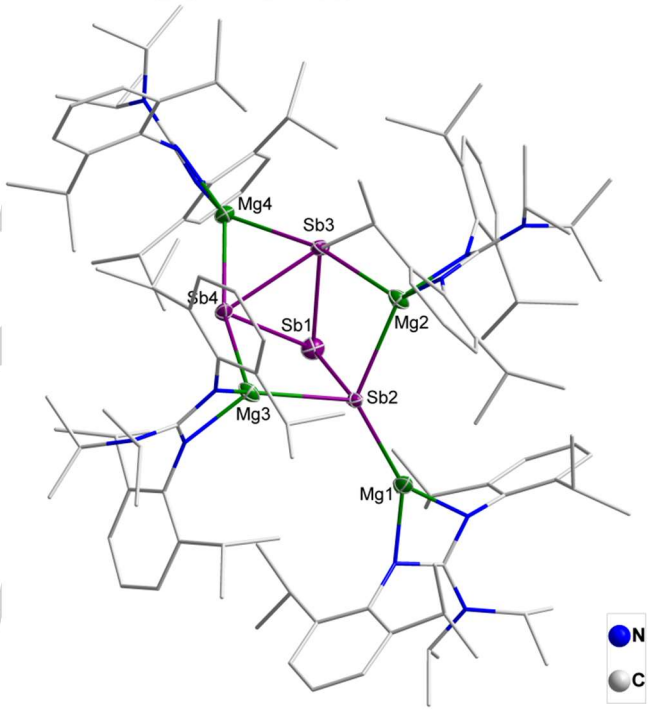

Figure 1. Molecular structure of $[(L^1Mg)_4Sb_4]$ **1**. H-atoms, lattice solvent and disordered Sb atoms have been omitted for clarity. Displacement ellipsoids of Sb and Mg are drawn at the 50% probability level and L^1 ligands are drawn in a wireframe format. Selected bond lengths (Å) and angles (°): Sb1-Sb2 2.8410(5), Sb1-Sb3 2.8352(5), Sb1-Sb4 2.8248(5), Sb3-Sb4 2.8847(5), Mg1-Sb2 2.7019(17), Mg2-Sb2 2.8050(16), Mg2-Sb3 2.8234(17), Mg3-Sb2 2.8444(16), Mg3-Sb4 2.7999(16), Mg4-Sb3 2.7600(17), Mg4-Sb4 2.7576(16); Sb2-Sb1-Sb3 89.959(13), Sb2-Sb1-Sb4 90.223(13), Sb1-Sb3-Sb4 59.181(12), Sb3-Sb4-Sb1 59.535(13), Sb4-Sb1-Sb3 61.284(13), Sb2-Mg2-Sb3 90.94(5), Sb2-Mg3-Sb4 90.66(4), Sb3-Mg4-Sb4 63.04(4), Mg1-Sb2-Sb1 99.22(4), Mg1-Sb2-Mg2 128.53(5), Mg1-Sb2-Mg3 128.87(5), Mg2-Sb3-Mg4 164.28(5), Mg2-Sb3-Sb1 84.63(3), Mg2-Sb3-Sb4 106.84(3), Mg2-Sb2-Sb1 84.86(3), Mg2-Sb2-Mg3 102.55(5), Mg3-Sb2-Sb1 85.85(3), Mg3-Sb4-Mg4 160.31(5), Mg3-Sb4-Sb1 87.00(4), Mg3-Sb4-Sb3 104.46(3), Mg4-Sb4-Sb3 58.52(4), Mg4-Sb3-Sb4 58.44(4), Mg4-Sb4-Sb1 91.41(4), Mg4-Sb3-Sb1 91.14(4).

The values of the bonding parameters of the minor (~15%) component of the disorder show - in some cases significant – differences and can be found in the SI. The only structurally characterized magnesium polystibides $[(L^{2,3}Mg)_4(\mu,\eta^{2:2:2:2}\text{-}Sb_8)]$

Accepted Manuscript

(2.882(3)-3.007(3) Å for L^2; 2.8459(10)-2.9007(10) Å for L^3)[12] showed significantly elongated Mg-Sb bond lengths, whereas the Mg-Sb bond length in $[\{Me_2SiSi(SiMe_3)_2\}_2SbMgBr(OEt_2)_2]$ (2.7806(13) Å) is comparable to those observed in **1**.[18] The bridging Sb-Mg-Sb angles in **1** vary significantly between 63.04(4)° (Sb3-Mg4-Sb4) and 90.94(5)° (Sb2-Mg2-Sb3). The Sb3-Sb4 bond (2.8847(5) Å) in the Sb_3 ring (Sb1-Sb3-Sb4) is slightly longer than the Sb1-Sb3 (2.8352(5) Å) and Sb1-Sb4 (2.8248(5) Å) bonds. The Sb2 atom adopts a position above the Sb_3 triangle and the Sb1-Sb2 (2.8410(5) Å) bond is perpendicular to the plane of the triangle (Sb2-Sb1-Sb3 89.96(2)°, Sb2-Sb1-Sb4 90.22(2)°). The endocyclic bond angles of the Sb_3 triangle are close to 60° (Sb1-Sb3-Sb4 59.18(2)°, Sb1-Sb4-Sb3 59.54(2)°, Sb3-Sb1-Sb4 61.28(2)°). Even though the arrangement of the four Sb atoms in **1** is without precedence for Sb clusters, it has been previously observed in analogous P_4 and As_4 complexes such as $[(CAAC)P_4((CH_3)CH_2C{=}CCH_2(CH_3))]$ (CAAC = alkyl(amino)carbene),[19a] $[(Cp_2Zr)P_4(PR_2)_2]$ (R = $SiMe_3$),[19b,c] $(Ter)_2Cl_2P_4$ (Ter = 2,6-dimesitylphenyl)[19d] and $[(Mes_2Si\text{-}SiMes_2)_2(As_4)]$,[19e] respectively.

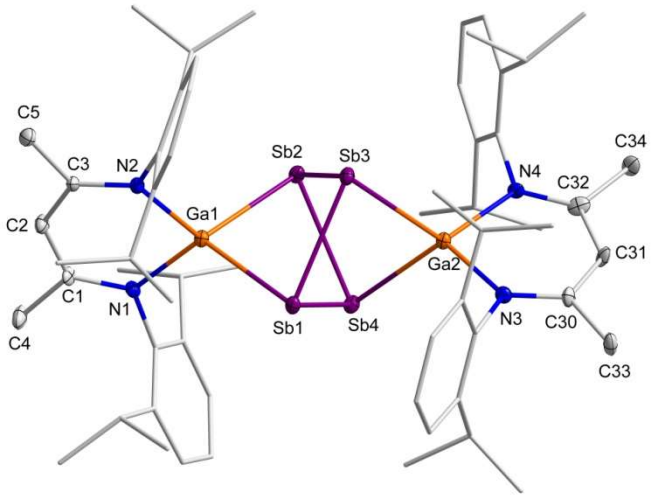

Figure 2. Molecular structure of $[(L^2Ga)_2Sb_4]$ **2**. H-atoms have been omitted for clarity and displacement ellipsoids are drawn at the 30% probability level. 2,6-*i*-Pr_2-C_6H_3 groups are drawn in wireframe format for simplicity. Selected bond lengths (Å) and angles (°): Sb1-Sb3 2.8500(9), Sb1-Sb4 2.8675(7), Sb2-Sb3 2.8683(8), Sb2-Sb4 2.8722(8), Ga1-Sb1 2.6637(11), Ga1-Sb2 2.6748(11), Ga2-Sb3 2.6676(11), Ga2-Sb4 2.6779(11); Sb1-Sb3-Sb2 81.86(2), Sb1-Sb4-Sb2 81.49(2), Sb3-Sb2-Sb4 80.79(2), Sb3-Sb1-Sb4 81.19(2), Sb1-Ga1-Sb2 89.13(3), Sb3-Ga2-Sb4 88.21(3), Ga1-Sb1-Sb3 79.08(3), Ga1-Sb1-Sb4 80.30(3), Ga1-Sb2-Sb4 80.03(3), Ga1-Sb2-Sb3 78.57(3), Ga2-Sb3-Sb1 79.84(3), Ga2-Sb3-Sb2 80.58(3), Ga2-Sb4-Sb1 79.35(3), Ga2-Sb4-Sb2 80.33(3).

The solid-state structure of **2**, which contains a folded Sb_4 cyclic unit with opposite ends bridged by two L^2Ga moieties, is similar to those of $[(L^2Al)_2(\mu,\eta^{2:2}\text{-}P_4)]$[20] and $[(L^4Si)_2(\mu,\eta^{2:2}\text{-}P_4)]$ (L^4 = $CH[(C{=}CH_2)CMe][N(2,6\text{-}i\text{-}Pr_2C_6H_3)]_2$),[21] which were synthesized by oxidative addition reactions of Al^I and Si^{II} species with white phosphorous (P_4), as well as $[(L^2Ga)_2(\mu,\eta^{2:2}\text{-}Ge_4)]$,[22] respectively. The Ga atoms in **2** adopt distorted tetrahedral geometry, whereas the Sb atoms show a pyramidal coordination sphere. The C_3N_2Ga rings of **2** are almost planar (rms deviation from the best planes 0.0603 and 0.0548 Å) as was observed for L^2Ga. In contrast, the bite angles (93.9(3)° N1-Ga1-N2, 94.1(3)° N3-Ga2-N4) of the chelating β-diketiminate ligands are larger and the Ga-N bond lengths (1.974(7)-2.004(7) Å) in **2** are shorter than those in the starting reagent L^2Ga (87.53(5)°, 2.0528(14) Å, 2.0560(13) Å).[14a] Shortening of the Ga-N bond usually occurs when the electron lone pair of L^2Ga^I is oxidatively added or inserted into any organic and inorganic derivatives.[23] The four independent Ga-Sb bond distances are virtually the same (Ga1-Sb1 2.6637(11), Ga1-Sb2 2.6748(11), Ga2-Sb3 2.6676(11), Ga2-Sb4 2.6779(11) Å) and comparable to those observed in the Ga-stabilized distibene $L^2(Me_2N)GaSb{=}SbGa(NMe_2)L^2$ (2.6200(4) Å), the Sb-analogue bicyclo[1.1.0]butane, $[\{L^2(Me_2N)Ga\}_2(\mu,\eta^{1:1}\text{-}Sb_4)]$ (2.5975(5) Å)[11] and in Ga-Sb σ-bonded compounds such as $[(dmap)Et_2GaSb(SiMe_3)_2]$ (2.648(1) Å; dmap = 4-dimethylamino pyridine)[24] and $[Me_2GaSbR'_2]_3$ (R' = $SiMe_3$, 2.6773(5)-2.7144(5) Å; Me, 2.666(1)-2.682(1) Å; *i*-Pr, 2.669(1)-2.694(1) Å).[25,26]

Table 1. Comparison of bond lengths (Å) and angles (°) in the Sb_4 units of $[\{L^2(Me_2N)Ga\}_2(Sb_4)]$,[11] **1** and **2**.[a]

	$[\{L^2(Me_2N)Ga\}_2(Sb_4)]$	**1**	**2**
Sb_1-Sb_2	2.8139(4) (Sb1a-Sb3)	2.8847(5) (Sb3-Sb4)	2.8500(9) (Sb1-Sb3)
Sb_1-Sb_3	2.8298(4) (Sb1a-Sb2)	2.8352(5) (Sb3-Sb1)	2.8675(7) (Sb1-Sb4)
Sb_2-Sb_3	2.7920(5) (Sb3-Sb2)	2.8248(5) (Sb1-Sb4)	-
Sb_2-Sb_4	2.8139(4) (Sb3-Sb1)	-	2.8683(8) (Sb3-Sb2)
Sb_3-Sb_4	2.8298(4) (Sb2-Sb1)	2.8410(5) (Sb1-Sb2)	2.8722(8) (Sb4-Sb2)
Sb_2-Sb_1-Sb_3	59.300(13) (Sb3-Sb1a-Sb2)	59.181(12) (Sb4-Sb3-Sb1)	81.19(2) (Sb3-Sb1-Sb4)
Sb_1-Sb_2-Sb_3	60.636(11) (Sb1a-Sb3-Sb2)	59.535(13) (Sb3-Sb4-Sb1)	-
Sb_1-Sb_3-Sb_2	60.065(11) (Sb1a-Sb2-Sb3)	61.284(13) (Sb3-Sb1-Sb4)	-
Sb_1-Sb_3-Sb_4	75.084(14) (Sb1a-Sb2-Sb1)	89.959(13) (Sb3-Sb1-Sb2)	81.49(2) (Sb1-Sb4-Sb2)
Sb_2-Sb_3-Sb_4	60.065(11) (Sb3-Sb2-Sb1)	90.223(13) (Sb4-Sb1-Sb2)	-
Sb_3-Sb_2-Sb_4	60.635(11) (Sb2-Sb3-Sb1)	-	-
Sb_2-Sb_4-Sb_3	59.300(13) (Sb3-Sb1-Sb2)	-	80.79(2) (Sb3-Sb2-Sb4)
Sb_1-Sb_2-Sb_4	75.585(14) (Sb1a-Sb3-Sb1)	-	81.86(2) (Sb1-Sb3-Sb2)

[a] Ideal Sb_4 tetrahedron: Sb-Sb 2.80 Å, Sb-Sb-Sb 60°.[17]

Accepted Manuscript

The Sb-Sb-Sb angles (table 1) within the Sb_4 ring in **2** vary from 80.79(2) to 81.86(2)°. The transannular Sb-Sb distances (Sb1-Sb2 3.7461(8) Å, Sb3-Sb4 3.7203(8) Å) in **2** indicate no significant bonding interactions. The dihedral angle (fold angle) between the two three-membered Sb rings is 61.40(2)° (Sb1/Sb3/Sb4, Sb2/Sb3/Sb4). The Sb-Sb bond lengths are similar for **1** (2.8248(5)-2.8847(5) Å) and **2** (2.8500(9)-2.8722(8) Å) and their values are comparable to those found in the cationic Sb_4 clusters, $[(R_3P)_4Sb_4][OTf]_4$ (2.8354(6)-2.8797(5) Å, R = Me; 2.838(2)-2 .884(2) Å, R = Et), $[(Me_3P)_3Sb_4R^2]$ (2.8209(5)-2.8612(5) Å)[10b,c], neutral R_4Sb_4 rings (2.814-2-887 Å, mean 2.85(2) Å),[27] anionic Sb chalcogenides $[Sb_6S_6]^{2-}$ (2.829(2)-2.871(2) Å), $[Sb_4S_6]^{2-}$ (2.8597(9) Å),[28] $[Sb_4Te_4]^{4-}$ (2.836(4)-2.883(4) Å) and $[Sb_9Te_6]^{3-}$ (2.756(5)-2.871(5) Å)[29] as well as the homopolyatomic anions Sb_4^{2-} (av. 2.750 Å) and Sb_7^{3-} (av. 2.797 Å),[30] respectively.

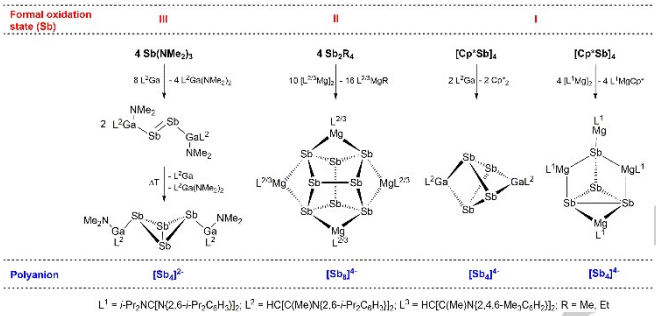

Scheme 2. Reactions of Sb(III), Sb(II) and Sb(I) compounds with one-electron (LMg) and two-electron reductants (LGa). Sb_4 units in $[\{L^2(Me_2N)Ga\}_2(Sb_4)]$, **1** and **2** and Sb_8 units observed in $[\{L^{2,3}Mg\}_4(Sb_8)]$.

The structure of the Sb_4 units in **1** and **2** can be derived from the neutral Sb_4 tetrahedron, in which either the L^1Mg^+ (**1**) or the L^2Ga^{2+} (**2**) fragments are inserted into two adjacent [1, 2] or two opposite [1, 4] edges of the tetrahedral Sb_4 unit, respectively (Fig. 3). In contrast, the previously reported Sb analogue of bicyclo[1,1,0]butane, $[\{L^2(Me_2N)Ga\}_2Sb_4]$, contains a $[Sb_4]^{2-}$ dianion,[11] which originates formally from the bond breakage of only one Sb-Sb bond of an Sb_4 tetrahedron. These type of homopolyatomic anions have also been reported for phosphorus and arsenic, but these complexes were typically obtained from activation reaction of either P_4 or As_4. In contrast, the Sb complexes are formed by reduction of a molecular metal organic Sb compounds and their formation strongly relies on the starting Sb compound, i.e. its formal oxidation state, and the reducing potential of the one- or two-electron reductant (scheme 2). This can clearly be seen when comparing the reactions of distibines Sb_2R_4 with L^2Ga, which proceeded with insertion of the Ga(I) compound in the Sb-Sb bond and subsequent formation of $L^2Ga(SbR_2)_2$,[13] whereas the reaction of Sb_2R_4 with the stronger reductant LMg yielded the $[Sb_8]^{4-}$ tetraanion.[12]

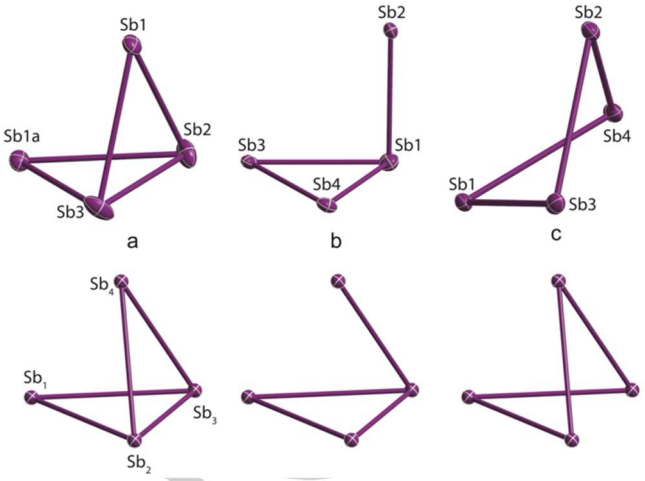

Figure 3. Sb_4 units in a) $[\{L^2(Me_2N)Ga\}_2(Sb_4)]$, b) **1** and c) **2**, displacement ellipsoids are drawn at the 30% probability level. Bottom: Models of [1], [1, 2] and [1, 4] edge-missing ideal tetrahedra.

The bonding situations in the Mg_4Sb_4 and Ga_2Sb_4 skeletons of **1** and **2** were further analyzed by using a number of quantum chemical techniques to gain further insight into their bonding situation and also compared to that of $[\{L^2(Me_2N)Ga\}_2(Sb_4)]$.[11] For **1**, two isomers $[(L^1Mg)_4Sb_4]$ (**I**) and $[(L^1Mg)_4Sb_4]$ (**II**) were found, from which isomer (**I**) is lower in energy by 6.7 kcal/mol at the ZORA-B3LYP-D3/TZP//BP86-D3/def2-SVP + ΔZPE level of theory (Fig. S15).[31-38] All calculated bond lengths within the Mg_4Sb_4 (isomer **I**) and Ga_2Sb_4 skeletons (Tables S2,S3) agree well with the corresponding experimental values (Δ*r* = 0.02–0.09 Å). The Sb–Sb bonds in **1** and **2** are covalent according to AIM, ELF, and NBO analyses (Tables S2,S3, Figures 4,5),[39-42] which agrees with previous computational results.[12,43] However, C_2-symmetrical **2** contains almost equivalent Sb–Sb bonds (2.925–2.959 Å), while the Sb–Sb bonds in **1** range from 2.852 to 2.974 Å. The elongated Sb3–Sb4 bond has smaller occupation number (ON; 1.89 |*e*|) and ELF basin population ($\bar{N}$ [V(Sb3,Sb4)] = 0.7 *e*) compared to other Sb–Sb bonds (ON=1.91–1.94 |*e*|; $\bar{N}$ [V(Sb,Sb)]=1.2–1.4 *e*). The Mg–Sb bonds have a mixed ionic/covalent character with a dominant ionic contribution as was found for the Mg–Sb bonds in $[(LMg)_4Sb_8]$.[12] Indeed, AIM parameters (Table S2) indicate an *intermediate* character of the Mg–Sb bonds ($\nabla^2\rho(\mathbf{r}_b)$ >0; $1<|V(\mathbf{r}_b)|/G(\mathbf{r}_b)<2$, $H(\mathbf{r}_b)<0$), while NBO analysis finds no covalent Mg–Sb bonds. Although ELF distribution (Fig. 4) reveals eight valence disynaptic V(Mg,Sb) basins implying some extent of covalent bonding, they are mainly formed by Sb lone pairs with a small contribution of the Mg atoms into populations of these ELF basins according to ELF/AIM intersection procedure ($\bar{N}$ [V(Mg,Sb)|Mg] = 0.1 *e*; V(Mg,Sb)≈V(Sb); Table S4).[44] In addition, NPA partial charges indicate strongly polarized Mg–Sb bonds with Sb atoms in three different formal oxidation states. The Mg1–Sb2 bond includes both the most positive (*q*(Mg1)=+1.34 |*e*|) and the most negative (*q*(Sb2)=-1.16 |*e*|) atoms within the Mg_4Sb_4 core, whereas the remaining Mg (+1.15/+1.16/+1.17 |*e*|) and Sb atoms (+0.19/-0.44/-0.51 |*e*|) carry less positive (Mg) and negative (Sb) charges. Although the

Accepted Manuscript

NBO analysis predicts eight lone pairs on Sb atoms in total with ON ranging between 1.6 and 2.0 |*e*|, ELF discloses the only one pure V(Sb) valence monosynaptic basin populated by 3.1 *e*, which is associated with the lone pair localized on Sb1 (Fig. 4d).

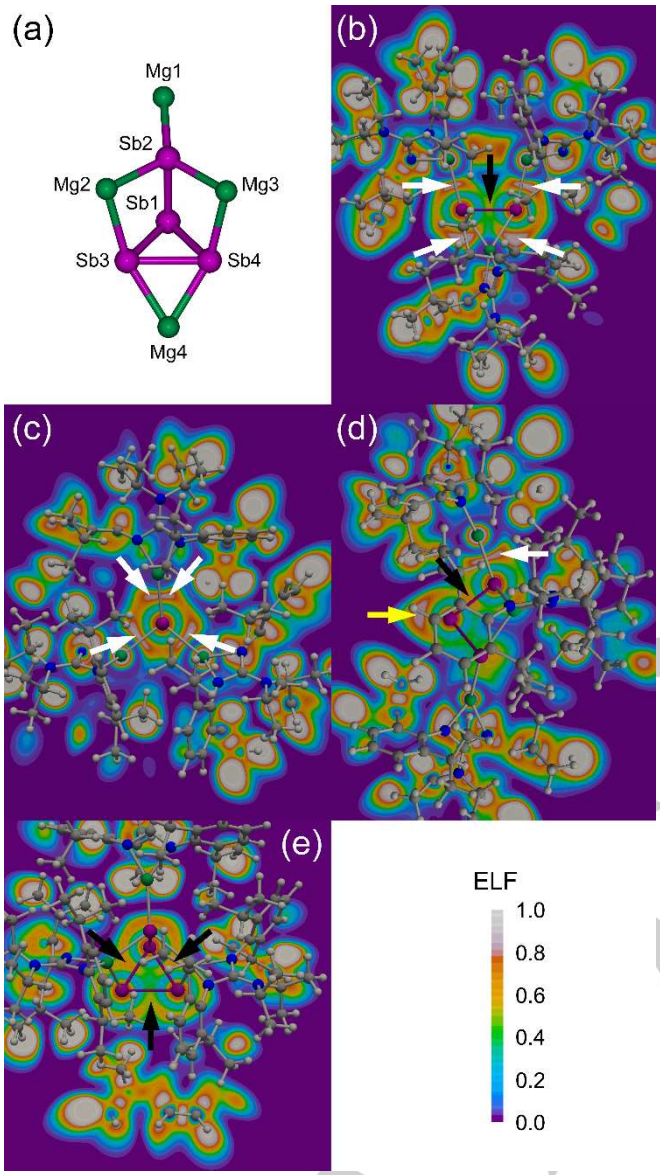

Figure 4. Atomic labeling for the Mg_4Sb_4 skeleton (a) and ELF distribution in $[(L^1Mg)_4Sb_4]$ (**I**) complex in the Mg2–Sb3–Sb4 (b), Mg1–Mg2–Mg3 (c), Mg1–Sb2–Sb1 (d), and Sb1–Sb3–Sb4 (e) planes. V(Mg,Sb), V(Sb), and V(Sb,Sb) basins are indicated by white (b, c, d), yellow (d), and black (b, d, e) arrows.

The Ga–Sb bonds are covalent, which is supported by the high contribution of Ga's electrons into the V(Ga,Sb) basins ($\bar{N}$ [V(Ga,Sb)|Ga] = 1.0 *e*), the presence of two-center two-electron $\sigma_{Ga–Sb}$ bonds (ON=1.93 |e|) with noticeable values of polarization coefficients ($|c_X|^2$=38–39%), *shared*–type Ga–Sb interactions ($\nabla^2\rho(\mathbf{r}_b) \leq 0$; $|V(\mathbf{r}_b)|/G(\mathbf{r}_b) \geq 2$, $H(\mathbf{r}_b) < 0$), and NPA charges (q(Ga)=+0.77 |e|, q(Sb)=-0.13/-0.14 |e|). These findings are in contrast to those reported for $[(L^2Al)_2P_4]$,[20] in which the Al-P bonds were described as highly polar (ionic), resulting from the higher electronegativity difference between Al and P compared to Ga and Sb. In addition, each Sb atom in **2** carries one electron lone pair as shown by NBO analysis (ON=2.0 |e|; Table S3) and ELF ($\bar{N}$ [V(Sb)]=1.4 *e*; Fig. 5).

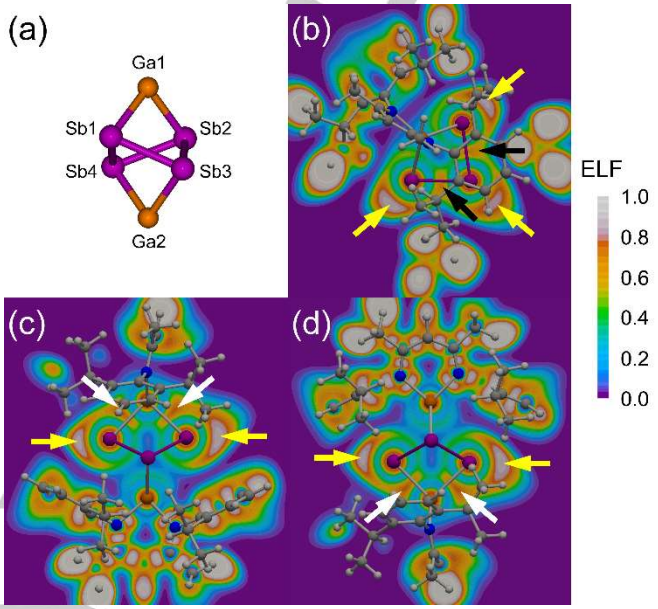

Figure 5. Atomic labeling for the Ga_2Sb_4 skeleton (a) and ELF distribution in $[(L^2Ga)_2Sb_4]$ complex in the Sb1–Sb2–Sb4 (b), Ga1–Sb1–Sb2 (c), and Ga2–Sb3–Sb4 (d) planes. V(Ga,Sb), V(Sb), and V(Sb,Sb) basins are indicated by white (c, d), yellow (b, c, d), and black (b) arrows.

Finally, the chemical bonding picture was analyzed in the Ga_2Sb_4 core of previously reported $[\{L^2(Me_2N)Ga\}_2Sb_4]$ compound,[11] which contains slightly shorter Ga–Sb (2.647/2.652 Å) and Sb–Sb distances (2.837-2.908 Å) compared to **2** (Table S4). According to our computational results, the bonding situation within the Ga_2Sb_4 unit is similar to that of **2** and is characterized by the covalent $\sigma_{Sb–Sb}$ and $\sigma_{Ga–Sb}$ bonds and four Sb lone pairs. However, in contrast to **2**, the Ga–Sb bonds are less polar ($\bar{N}$ [V(Ga,Sb)|Ga]=1.2 *e*; $|c_X|^2$=41%). In addition, the skeleton includes five Sb–Sb bonds and two Sb atoms are positively charged (q(Sb2)=+0.06 |e|, q(Sb3)=+0.03 |e|).

Conclusions

In summary, the anionic and neutral Sb_4 clusters **1** and **2** were obtained from the reactions of $[Cp^*Sb]_4$ with two electron reductants, $[L^1Mg]_2$ and L^2Ga. Both reactions follow distinct pathways and formation of **1** and **2** occurs through the elimination of L^1MgCp^* and Cp^*_2. The structure of the Sb_4 units in **1** and **2** can be derived from the neutral Sb_4 tetrahedron, in which either the L^1Mg^+ (**1**) or the L^2Ga^{2+} (**2**) fragments are inserted into two adjacent [1, 2] or two opposite [1, 4] edges of the tetrahedral Sb_4 unit, respectively. **1**, **2** and $[\{L^2(Me_2N)Ga\}_2(\mu,\eta^{1:1}\text{-}Sb_4)]$[11] are promising candidates for the synthesis of the neutral Sb_4 tetrahedron,

Accepted Manuscript

which was only structurally characterized using scanning tunneling microscope (STM) in vapor phase deposited Sb thin films.[45]

Experimental Section

General Procedures. The reactions were carried out in purified argon atmosphere using standard Schlenk and glove-box techniques. Benzene was carefully dried over sodium and hexane was collected from m-Braun solvent purification system. Deuterated solvents were stored over activated molecular sieves (4 Å) and degassed prior to use. Karl Fischer titration of the dry solvents showed values below 3 ppm. The compounds $[L^1Mg]_2$ {L^1 = *i*-$Pr_2NC[N(2,6\text{-}i\text{-}Pr_2C_6H_3)]_2$[16], L^2Ga {L^2 = $HC[C(Me)N(2,6\text{-}i\text{-}Pr_2C_6H_3)]_2$}[14a] and $[Cp^*Sb]_4$[46] were prepared by following literature methods. $[Cp^*Sb]_4$ was crystallized from benzene at 8 °C and the ^{1}H NMR spectrum shows a single peak at 1.92 ppm in benzene-d_6 (Fig. S13). Other chemicals were obtained from commercial sources and purified prior to use. While drying the compound at high vacuum (1×10^{-3} mmHg), **1** decomposed significantly into black precipitate. In order to avoid the decomposition, the reaction work-up was carried out in argon filled glove-box.

Instrumentation. The ^{1}H (300 MHz) and $^{13}C\{^1H\}$ (75.5 MHz or 150 MHz) NMR (δ in ppm) spectra were recorded using a Bruker Avance DPX-300 or Bruker Avance III HD spectrometers and the spectra were referenced to internal C_6D_5H (^{1}H: δ = 7.154; ^{13}C: δ = 128.39) and $C_6D_5CHD_2$ (^{1}H: δ = 2.09; ^{13}C: δ = 20.40). The microanalyses were performed at the elemental analysis laboratory of University of Duisburg-Essen. IR spectra were measured in an ALPHA-T FT-IR spectrometer equipped with a single reflection ATR sampling module. The spectrometer was placed in a glovebox so as to perform the FT-IR measurements in inert gas atmosphere. SEM and EDX was measured using a Jeol JSM 6510 equipped with a Bruker Quantax 400 device.

Synthesis of 1. In an J-Young NMR tube, a mixture of $[L^1Mg]_2$ (68 mg, 0.070 mmol) and $[Cp^*Sb]_4$ (18 mg, 0.0175 mmol) was taken in 0.5 mL of benzene-d_6. The solution was stirred at room temperature for 3 days and kept at 8 °C. The reaction mixture afforded a mixture of red (**1**) and colorless (L^1MgCp^*) crystals after 3 days. The solution was decanted and the colorless crystals are washed-out with benzene (3 × 0.5 mL) to afford pure form of **1**. Yield: 24 mg (0.0197 mmol, 56 %). Anal. Calcd. for $C_{124}H_{192}N_{12}Mg_4Sb_4$: C, 61.16; H, 7.95; N, 6.90. Found: C, 61.70; H, 7.87; N, 6.81 %. IR (neat): ν 2963, 2872, 1616, 1580, 1458, 1427, 1372, 1323, 1281, 1244, 1177, 1116, 1049, 946, 928, 873, 800, 751, 721, 660, 598, 519, 416 cm^{-1}. ^{1}H NMR (C_6D_6, 300 MHz): δ 7.14-7.06 (m, 6 H, $C_6H_3(^iPr)_2$), 3.97 (sept, 2 H, *J* = 6.9 Hz, -NC*H*$(CH_3)_2$), 3.56 (two sept, 4 H, -ArC*H*$(CH_3)_2$), 1.35 (d, 3 H, *J* = 6.6 Hz, -ArCH(C*H*$_3)_2$), 1.34 (d, 3 H, *J* = 6.6 Hz, -ArCH(C*H*$_3)_2$), 1.30 (d, 9 H, *J* = 6.9 Hz, -ArCH(C*H*$_3)_2$), 0.98 (d, 9 H, *J* = 6.6 Hz, -ArCH(C*H*$_3)_2$), 0.77 (d, 12 H, *J* = 6.9 Hz, -NCH(C*H*$_3)_2$). ^{13}C NMR (C_6D_6, 150 MHz): δ 167.59 (N$_3$*C*), 144.18 (C_6H_3), 143.41 (C_6H_3), 143.03 (C_6H_3), 123.80 (C_6H_3), 123.46 (C_6H_3), 123.39 (C_6H_3), 50.06 & 49.97 (NC*H*$(CH_3)_2$), 28.26 (-ArCH(*C*H$_3)_2$), 28.15 (-ArCH(*C*H$_3)_2$), 27.89 (-ArCH(*C*H$_3)_2$), 27.29 (-ArCH(*C*H$_3)_2$), 24.02 (-NCH(*C*H$_3)_2$), 23.98 (-NCH(*C*H$_3)_2$), 22.77 (-ArCH(CH$_3$)$_2$), 22.68 (-ArCH(*C*H$_3)_2$).

Synthesis of 2. In an J-Young NMR tube, a mixture of L^2Ga (28 mg, 0.0584 mmol) and $[Cp^*Sb]_4$ (30 mg, 0.0292 mmol) was taken in 0.5 mL of benzene-d_6. The solution was heated at 71 °C and the reaction progress was monitored periodically using ^{1}H NMR spectroscopy. Within 3 days the resonances corresponding to L^2Ga and $[Cp^*Sb]_4$ vanished and a red solution was formed, which was then cooled to room temperature and transferred to 25 mL Schlenk tube. The solvents were removed under reduced pressure and the residue was dissolved in 2 mL of warm hexane. Storage of the red solution at 8 °C for 2 days leads to red crystals of **2**. Yield: 17 mg (0.0116 mmol, 40 %). Anal. Calcd. for $C_{58}H_{82}N_4Ga_2Sb_4$: C, 47.66; H, 5.65; N, 3.83. Found: C, 47.90; H, 5.73; N, 3.97 %. IR (neat): ν 3064, 2959, 2924, 2866, 1552, 1529, 1465, 1436, 1395, 1314, 1256, 1174, 1098, 1017, 930, 849, 796, 755, 628, 523, 447 cm^{-1}. ^{1}H NMR (C_6D_6, 500 MHz): δ 7.11 (s, 6 H, $C_6H_3(^iPr)_2$), 4.75 (s, 1 H, γ-C*H*-), 3.72 (sept, 4 H, -C*H*$(CH_3)_2$), 1.64 (s, 6 H, ArNCC*H*$_3$), 1.54 (d, 12 H, *J* = 6.5 Hz, -CH(C*H*$_3)_2$), 1.10 (d, 12 H, *J* = 6.5 Hz, -CH(C*H*$_3)_2$). ^{13}C NMR (C_6D_6, 150 MHz): δ 167.59 (ArN*C*CH$_3$), 144.47 (C_6H_3), 144.67 (C_6H_3), 128.68 (C_6H_3), 127.71 (C_6H_3), 125.00 (C_6H_3), 95.15 (γ-CH-), 30.01 (-*C*H$(CH_3)_2$), 25.83 (-CH(*C*H$_3)_2$), 24.59 (-CH(*C*H$_3)_2$), 24.49 (ArNC*C*H$_3$).

Single Crystal X-ray diffraction. The crystals were mounted on nylon loops in inert oil. Data were collected on a Bruker AXS D8 Kappa diffractometer with APEX2 detector (monochromated Mo$_{K\alpha}$ radiation, λ = 0.71073 Å). The structures were solved by Direct Methods (SHELXS-97) and refined anisotropically by full-matrix least-squares on F^2 (SHELXL-2014).[47] Absorption corrections were performed semi-empirically from equivalent reflections on basis of multi-scans (**1**) and numerical from indexed faces (**2**) (Bruker AXS APEX2). Hydrogen atoms were refined using a riding model or rigid methyl groups. In **1** the Sb core of the complex is disordered over two positions. The rather high values of the ADP of the benzene molecules suggest minor disorders which could not be resolved to two components. The bond lengths and angles of the solvent molecules should be considered meaningless and the ones of the Sb core carefully assessed. The absolute structure could be determined reliably. Parsons quotient method was used to determine the absolute structure parameter x.[48]

Computational details. The geometric parameters of the species under study were fully optimized in the gas phase at the BP86-D3/def2-SVP theoretical level[31–34] with a corresponding small-core relativistic effective core potential for Sb[35] employing ultrafine grid. The stationary points were characterized as minima on the potential energy surface by vibrational analysis (the number of imaginary frequencies (NImag) was equal to zero) and the structures obtained were used for the subsequent calculations. Zero-point vibrational energies (ZPEs) were computed from the BP86-D3/def2-SVP harmonic vibrational frequencies without scaling factors. The thermal corrections to the enthalpy and to the Gibbs free energy were calculated within the rigid-rotor–harmonic-oscillator approximation and used for obtaining ΔH^0_{298} and ΔG^0_{298} values. To obtain more accurate relative energies of isomers, single-point scalar relativistic (SR) ZORA-B3LYP-D3/TZP computations[36–38] were additionally carried out. Atoms in molecules (AIM)[39] and electron localization function (ELF)[40,41] computations were performed with DGrid program[49] using densities from the all-electron SR-ZORA-BP86-D3/TZP computations. ELF basin populations were calculated for a rectangular parallelepipedic grid with a mesh size of 0.1 bohr. The natural bond orbital analysis (NBO)[40] was performed at the BP86-D3/def2-SVP theoretical level as implemented in Gaussian09. SR-ZORA-BP86-D3/TZP and SR-ZORA-B3LYP-D3/TZP computations were performed using ADF2013 suite of programs (core potentials were not used, and quality of the Becke numerical integration grid was set to the keyword *good*),[50–52] while the remaining computations were carried out in Gaussian09 code.[53] Detailed information about AIM, ELF, and NBO can be found elsewhere.[39-42].

Acknowledgements

Financial support by the Deutsche Forschungsgemeinschaft (SCHU 1069/22-1) and the Russian Science Foundation (Grant No. 14-23-00013, A.S.N.) is acknowledged. The Siberian Supercomputer Center is acknowledged for providing computational resources.

Accepted Manuscript

Keywords: Main group elements • Zintl ions • Cluster compounds • Subvalent compounds

[1] For review articles see: a) S. Scharfe, F. Kraus, S. Stegmaier, A. Schier, T. F. Fässler, *Angew. Chem.* **2011**, *123*, 3712–3754; *Angew. Chem. Int. Ed.* **2011**, *50*, 3630–3670; b) R. S. P. Turbervill, J. M. Goicoechea, *Chem. Rev.* **2014**, *114*, 10807–10828.

[2] a) M. A. Beswick, N. Choi, C. N. Harmer, A. D. Hopkins, M. McPartlin, D. S. Wright, *Science* **1998**, *281*, 1500–1501; b) A. Bashall, M. A. Beswick, N. Choi, A. D. Hopkins, S. J. Kidd, Y. G. Lawson, M. E. G. Mosquera, M. McPartlin, P. R. Raithby, A. A. E. H. Wheatley, J. A. Wood, D. S. Wright, *Dalton Trans.* **2000**, 479–486; c) H. J. Breunig, M. E. Ghesner, E. Lork, *Z. Anorg. Allg. Chem.* **2005**, *631*, 851–856.

[3] a) W. Huang, P. L. Diaconescu, *Chem. Commun*. **2012**, *48*, 2216–2218; b) S. N. Konchenko, N. A. Pushkarevsky, M. T. Gamer, R. Köppe, H. Schnöckel, P. W. Roesky, *J. Am. Chem. Soc*. **2009**, *131*, 5740–5741; c) T. Li, S. Kaercher, P. W. Roesky, *Chem. Soc. Rev*. **2014**, *43*, 42–57.

[4] S. Heinl, M. Scheer, *Chem. Sci.* **2014**, *5*, 3221–3225.

[5] C. Schwarzmaier, A. Y. Timoshkin, G. Balázs, M. Scheer, *Angew. Chem.* **2014**, *126*, 9223–9227; *Angew. Chem. Int. Ed*. **2014**, *53*, 9077–9081 and references cited therein.

[6] M. Arrowsmith, M. S. Hill, A. L. Johnson, G. Kociok-Köhn, M. F. Mahon, *Angew. Chem.* **2015**, *127*, 7993–7996; *Angew. Chem. Int. Ed.* **2015**, *54*, 7882–7885.

[7] a) J. E. Borger, A. W. Ehlers, M. Lutz, J. C. Slootweg, K. Lammertsma, *Angew. Chem.* **2014**, *126*, 13050–13053; *Angew. Chem. Int. Ed.* **2014**, *53*, 12836–12839; b) J. E. Borger, A. W. Ehlers, M. Lutz, J. C. Slootweg, K. Lammertsma, *Angew. Chem.* **2016**, *128*, 623–627; *Angew. Chem. Int. Ed.* **2016**, *55*, 613–617.

[8] W. T. K. Chan, F. García, A. D. Hopkins, L. C. Martin, M. McPartlin, D. S. Wright, *Angew. Chem.* **2007**, *119*, 3144–3146; *Angew. Chem. Int. Ed.* **2007**, *46*, 3084–3086.

[9] a) F. Spitzer, M. Sierka, M. Latronico, P. Mastrorilli, A. V. Virovets, M. Scheer, *Angew. Chem.* **2015**, *127*, 4467–4472; *Angew. Chem. Int. Ed.* **2015**, *54*, 4392–4396; b) C. Schwarzmaier, M. Sierka, M. Scheer, *Angew. Chem.* **2013**, *125*, 891–894; *Angew. Chem. Int. Ed.* **2013**, *52*, 858–861; c) C. Schwarzmaier, A. Y. Timoshkin, M. Scheer, *Angew. Chem.* **2013**, *125*, 7751–7755; *Angew. Chem. Int. Ed.* **2013**, *52*, 7600–7603; d) C. Schwarzmaier, A. Schindler, C. Heindl, S. Scheuermayer, E. V. Peresypkina, A. V. Virovets, M. Neumeier, R. Gschwind, M. Scheer, *Angew. Chem.* **2013**, *125*, 11097–11100; *Angew. Chem. Int. Ed.* **2013**, *52*, 10896–10899; e) J. E. Borger, M. S. Bakker, A. W. Ehlers, M. Lutz, J. C. Slootweg, K. Lammertsma, *Chem. Commun.* **2016**, *52*, 3284–3287; f) G. Santiso-Quiñones, A. Reisinger, J. Slattery, I. Krossing, *Chem. Commun.* **2007**, 5046–5048; g) I. Krossing, *J. Am. Chem.* Soc. **2001**, *123*, 4603–4604.

[10] a) M. H. Holthausen, K. Feldmann, S. Schulz, A. Hepp, J. J. Weigand, *Inorg. Chem.* **2012**, *51*, 3374–3387; b) S. S. Chitnis, A. P. M. Robertson, N. Burford, J. J. Weigand, R. Fischer, *Chem. Sci.* **2015**, *6*, 2559–2574; c) S. S. Chitnis, Y.-Y. Carpenter, N. Burford, R. McDonald, M. J. Ferguson, *Angew. Chem.* **2013**, *125*, 4963–4966; *Angew. Chem. Int. Ed.* **2013**, *52*, 4863–4866; d) S. S. Chitnis, N. Burford, J. J. Weigand, R. McDonald, *Angew. Chem.* **2015**, *127*, 7939–7943; *Angew. Chem. Int. Ed.* **2015**, *54*, 7828–7832; e) M. Donath, E. Conrad, P. Jerabek, G. Frenking, R. Fröhlich, N. Burford, J. J. Weigand, *Angew. Chem.* **2012**, *124*, 3018–3021; *Angew. Chem. Int. Ed.* **2012**, *51*, 2964–2967; f) M. Donath, M. Bodensteiner, J. J. Weigand, *Chem. Eur. J.* **2014**, *20*, 17306–17310. g) M. Lindsjö, A. Fischer, L. Kloo, *Angew. Chem.* **2004**, *116*, 2594–2597; *Angew. Chem. Int. Ed.* **2004**, *43*, 2540–2543.

[11] L. Tuscher, C. Ganesamoorthy, D. Bläser, C. Wölper, S. Schulz, *Angew. Chem.* **2015**, *127*, 10803–10807; *Angew. Chem. Int. Ed.* **2015**, *54*, 10657–10661.

[12] C. Ganesamoorthy, C. Wölper, A. S. Nizovtsev, S. Schulz, *Angew. Chem.* **2016**, *128*, 4276–4281; *Angew. Chem. Int. Ed.* **2016**, *55*, 4204–4209.

[13] C. Ganesamoorthy, D. Bläser, C. Wölper, S. Schulz, *Angew. Chem.* **2014**, *126*, 11771–11775; *Angew. Chem. Int. Ed.* **2014**, *53*, 11587–11591.

[14] a) N. J. Hardman, B. E. Eichler, P. P. Power, *Chem. Commun.* **2000**, 1991; b) N. J. Hardman, P. P. Power, J. D. Gorden, C. L. B. Macdonald, A. H. Cowley, *Chem. Commun.* **2001**, 1866–1867; c) C. Ganesamoorthy, M. Matthias, D. Bläser, C. Wölper, S. Schulz, *Dalton Trans.* **2016**, 45, 11437–11444.

[15] **1**: $[C_{154}H_{222}Mg_4N_{12}Sb_4]$, M = 2825.66, orange crystal, (0.243 × 0.141 × 0.051 mm); monoclinic, space group $P2_1$; a = 15.3071(7) Å, b = 30.3372(15) Å, c = 18.0751(9) Å; α = 90°, β = 113.530(2)°, γ = 90°, V = 7695.7(7) Å^3; Z = 2; μ = 0.761 mm^{-1}; ρ_{calc} = 1.219 g·cm^{-3}; 146938 reflections (θ_{max} = 30.675°), 46811 unique (R_{int} = 0.0652); 1643 parameters; Flack-Parameter x = 0.003(5); largest max./min in the final difference Fourier synthesis 1.197 e·Å^{-3}/ -1.169 e·Å^{-3}; max./min. transmission 0.75/0.63; R_1 = 0.0460 (I > 2σ(I)), wR_2 = 0.1006 (all data). **2**: $[C_{58}H_{82}Ga_2N_4Sb_4]$, M = 1461.71, red crystal, (0.142 × 0.132 × 0.040 mm); orthorhombic, space group $P2_12_12_1$; a = 12.9684(8) Å, b = 15.2556(10) Å, c = 30.430(2) Å; α = 90°, β = 90°, γ = 90°, V = 6020.2(7) Å^3; Z = 4; μ = 2.689 mm^{-1}; ρ_{calc} = 1.613 g·cm^{-3}; 67988 reflections (θ_{max} = 30.598°), 17240 unique (R_{int} = 0.0586); 633 parameters; Flack-Parameter x = 0.037(7); largest max./min in the final difference Fourier synthesis 1.775 e·Å^{-3}/ -1.551 e·Å^{-3}; max./min. transmission 1.00/0.64; R_1 = 0.0497 (I > 2σ(I)), wR_2 = 0.1206 (all data). The crystallographic data of **1** and **2** (excluding structure factors) have been deposited with the Cambridge Crystallographic Data Centre as supplementary publication nos. CCDC- 1510376 (**1**), CCDC- 1510375 (**2**),. Copies of the data can be obtained free of charge on application to CCDC, 12 Union Road, Cambridge, CB21EZ (fax: (+44) 1223/336033; e-mail: deposit@ccdc.cam-ak.uk).

[16] S. P. Green, C. Jones, A. Stasch, *Science* **2007**, *318*, 1754–1757.

[17] P. Pyykkö, M. Atsumi, *Chem. Eur. J.* **2009**, *15*, 186–197.

[18] R. Zitz, J. Baumgartner, C. Marschner, *Organometallics* **2015**, *34*, 1431–1439.

[19] a) J. D. Masuda, W. W. Schoeller, B. Donnadieu, G. Bertrand, *Angew. Chem.* **2007**, *119*, 7182–7185; *Angew. Chem. Int. Ed.* **2007**, *46*, 7052–7055; b) E. Hey, M. F. Lappert, J. L. Atwood, S. G. Bott, *Chem. Commun.* **1987**, 597–598; c) A. Wisniewska, A. Łapczuk-Krygier, K. Baranowska, J. Chojnacki, E. Matern, J. Pikies, R. Grubba, *Polyhedron* **2013**, *55*, 45–48; d) J. Bresien, C. Hering, A. Schulz, A. Villinger, *Chem. Eur. J.* **2014**, *20*, 12607–12615; e) R. P. Tan, N. M. Comerlato, D. R. Powell, R. West, *Angew. Chem.* **1992**, *104*, 1251–1252; *Angew. Chem. Int. Ed.* **1992**, *31*, 1217–1218.

[20] Y. Peng, H. Fan, H. Zhu, H. W. Roesky, J. Magull, C. E. Hughes, *Angew. Chem.* **2004**, *116*, 3525–3527; *Angew. Chem. Int. Ed.* **2004**, *43*, 3443–3445.

[21] Y. Xiong, S. Yao, M. Brym, M. Driess, *Angew. Chem.* **2007**, *119*, 4595–4597; *Angew. Chem. Int. Ed.* **2007**, *46*, 4511–4513.

[22] A. Doddi, C. Gemel, M. Winter, R. A. Fischer, C. Goedecke, H. S. Rzepa, G. Frenking, *Angew. Chem.* **2013**, *125*, 468–472; *Angew. Chem. Int. Ed.* **2013**, *52*, 450–454.

[23] For L^{2}Ga derivatives see: a) M. Asay, C. Jones, M. Driess, *Chem. Rev.* **2011**, *111*, 354-396; b) C. J. Allan, C. L. B. Macdonald, Low-Coordinate Main Group Compounds – Group 13. *Comprehensive Inorganic Chemistry II, Vol 1.* Oxford: Elsevier; **2013**, p. 485–566; c) N. J. Hardman, A. D. Phillips, P. P. Power, *ACS Symp. Ser.* **2002**, *822*, 2–15.

[24] F. Thomas, S. Schulz, M. Nieger, *Eur. J. Inorg. Chem.* **2001**,161–166.

[25] A. Kuczkowski, S. Fahrenholz, S. Schulz, M. Nieger, *Organometallics* **2004**, *23*, 3615–3621.

[26] S. Schulz, M. Nieger, *J. Organomet. Chem.* **1998**, *570*, 275–278.

[27] Cambridge Structural Database, Version 5.37, see also: F.H. Allen, *Acta Cryst.* **2002**, *B58*, 380-388. Search for an Sb_4 ring with any atom bonded to the Sb atoms and the co-ordination number of the Sb set to

Accepted Manuscript

3. The results were limited to non-ionic compound which yielded 12 hits with 60 independent bonds.
[28] T. M. Martin, G. L. Schimek, W. T. Pennington, J. W. Kolis, *Dalton Trans.* **1995**, 501–502.
[29] C. J. Warren, D. M. Ho, R. C. Haushalter, A. B. Bocarsly, *Angew. Chem.* **1993**, *105*, 1684–1687; *Angew. Chem. Int. Ed.* **1993**, 32, 1646–1648.
[30] S. C. Critchlow, J. D. Corbett, *Inorg. Chem.* **1984**, *23*, 770-774.
[31] A. D. Becke, *Phys. Rev. A* **1988**, *38*, 3098–3100.
[32] J. P. Perdew, *Phys. Rev. B* **1986**, *33*, 8822–8824.
[33] S. Grimme, J. Antony, S. Ehrlich, H. Krieg, *J. Chem. Phys.* **2010**, *132*, 154104–154119.
[34] F. Weigend, R. Ahlrichs, *Phys. Chem. Chem. Phys.* **2005**, *7*, 3297–3305.
[35] B. Metz, H. Stoll, M. Dolg, *J. Chem. Phys.* **2000**, *113*, 2563–2569.
[36] E. van Lenthe, R. van Leeuwen, E. J. Baerends, *Int. J. Quantum Chem.* **1996**, *57*, 281–293.
[37] A. D. Becke, *J. Chem. Phys.* **1993**, *98*, 1372–1377.
[38] C. Lee, W. Yang, R. G. Parr, *Phys. Rev. B* **1988**, *37*, 785–789.
[39] R. F. W Bader, Atoms in Molecules: A Quantum Theory, Claredon Press: Oxford, U.K., 1990.
[40] A. E. Reed, L. A. Curtiss, F. Weinhold, *Chem. Rev.* **1988**, *88*, 899–926.
[41] A. D. Becke, K. E. Edgecombe, *J. Chem. Phys.* **1990**, *92*, 5397–5403.
[42] B. Silvi, A. Savin, *Nature* **1994**, *371*, 683–686.
[43] A. S. Nizovtsev, A. S. Ivanov, A. I. Boldyrev, S. N. Konchenko, *Eur. J. Inorg. Chem.* **2015**, *35*, 5801–5807.
[44] S. Raub, G. Jansen, *Theor. Chem. Acc.* **2001**, *106*, 223–232.
[45] T. M. Bernhardt, B. Stegemann, B. Kaiser, K. Rademann, *Angew. Chem.* **2003**, *115*, 209–212; *Angew. Chem. Int. Ed.* **2003**, *42*, 199–202.
[46] a) T. F. Berlitz, H. Sinning, J. Lorberth, U. Müller, *Z. Naturforsch.* **1988**, *43b,* 744–748; b) O. M. Kekia, R. L. Jones Jr., A. L. Rheingold, *Organometallics* **1996**, *15*, 4104–4106.
[47] a) G. M. Sheldrick, *Acta Crystallogr.* **1990**, *A46*, 467–473; b) G. M. Sheldrick, SHELXL-2014, Program for the Refinement of Crystal Structures University of Göttingen, Göttingen (Germany) **2014**; c) G. M. Sheldrick, *Acta Crystallogr.* **2008**, *A64*, 112–122); d) shelXle, *A Qt GUI for SHELXL*, C. B. Hübschle, G. M. Sheldrick, B. Dittrich, *J. Appl. Cryst.* **2011**, *44*, 1281–1284.
[48] For more details see: a) S. Parsons, H. D. Flack, *Acta Cryst.* **2004**, *A60*, s61; b) S. Parsons, H. D. Flack, T. Wagner, *Acta Cryst.* **2013**, *B69*, 249–259.
[49] M. Kohout, DGrid, version 4.6, Radebeul, 2011.
[50] ADF2013, SCM, Theoretical Chemistry, Vrije Universiteit, Amsterdam, The Netherlands, http://www.scm.com.
[51] C. F. Guerra, J. G. Snijders, G. te Velde, E. J. Baerends, *Theor. Chem. Acc.*, **1998**, *99*, 391–403.
[52] G. te Velde, F. M. Bickelhaupt, E. J. Baerends, C. Fonseca Guerra, S. J. van Gisbergen, J. G. Snijders, T. Ziegler, *J. Comput. Chem.*, **2001**, *22*, 931–967.
[53] M. J. Frisch, G. W. Trucks, H. B. Schlegel, G. E. Scuseria, M. A. Robb, J. R. Cheeseman, G. Scalmani, V. Barone, B. Mennucci, G. A. Petersson, H. Nakatsuji, M. Caricato, X. Li, H. P. Hratchian, A. F. Izmaylov, J. Bloino, G. Zheng, J. L. Sonnenberg, M. Hada, M. Ehara, K. Toyota, R. Fukuda, J. Hasegawa, M. Ishida, T. Nakajima, Y. Honda, O. Kitao, H. Nakai, T. Vreven, J. A. Montgomery, Jr., J. E. Peralta, F. Ogliaro, M. Bearpark, J. J. Heyd, E. Brothers, K. N. Kudin, V. N. Staroverov, R. Kobayashi, J. Normand, K. Raghavachari, A. Rendell, J. C. Burant, S. S. Iyengar, J. Tomasi, M. Cossi, N. Rega, J. M. Millam, M. Klene, J. E. Knox, J. B. Cross, V. Bakken, C. Adamo, J. Jaramillo, R. Gomperts, R. E. Stratmann, O. Yazyev, A. J. Austin, R. Cammi, C. Pomelli, J. W. Ochterski, R. L. Martin, K. Morokuma, V. G. Zakrzewski, G. A. Voth, P. Salvador, J. J. Dannenberg, S. Dapprich, A. D. Daniels, Ö. Farkas, J. B. Foresman, J. V. Ortiz, J. Cioslowski, D. J. Fox, Gaussian 09, Revision D.01; Gaussian, Inc.: Wallingford CT, 2013.

WILEY-VCH

Entry for the Table of Contents

Polystibides

*C. Ganesamoorthy, J. Krüger, C. Wölper, A. S. Nizovtsev and S. Schulz**

_____ *Page – Page*

Reduction of $[Cp^*Sb]_4$ with subvalent main group metal reductants - Syntheses and Structures of $[(L^1Mg)_4(Sb_4)]$ and $[(L^2Ga)_2(Sb_4)]$ containing edge-missing Sb_4 Units.

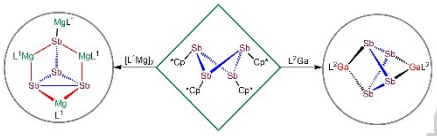

Go four Antimony: $[(L^1Mg)_4(\mu_4,\eta^{1:2:2:2}\text{-}Sb_4)]$ { L^1 = (N-*i*-Pr_2)C[N(2,6-$^i Pr_2C_6H_3$)]$_2$, **1**}, $[(L^2Ga)_2(\mu,\eta^{2:2}\text{-}Sb_4)]$ {L^2 = HC[C(Me)N(2,6-$^i Pr_2C_6H_3$)]$_2$, **2**} containing adjacent and opposite edge-missing Sb_4 tetrahedrons were obtained from reactions of $[Cp^*Sb]_4$ with $[L^1Mg]_2$ and L^2Ga. They were characterized by single crystal X-ray diffraction and their bonding situation investigated by quantum chemical calculations.

WILEY-VCH

DuEPublico

Duisburg-Essen Publications online

UNIVERSITÄT DUISBURG ESSEN

Offen im Denken

ub universitäts bibliothek

This text is made available via DuEPublico, the institutional repository of the University of Duisburg-Essen. This version may eventually differ from another version distributed by a commercial publisher.

DOI: 10.1002/chem.201605547
URN: urn:nbn:de:hbz:464-20201208-103739-9

This is the peer reviewed version of the following article: Ganesamoorthy, C.; Krüger, J.; Wölper, C.; Nizovtsev, A.S.; Schulz, S.: Reduction of [Cp*Sb]4 with Subvalent Main-Group Metal Reductants: Syntheses and Structures of [(L1Mg)4(Sb4)] and [(L2Ga)2(Sb4)] Containing Edge-Missing Sb4 Units. Chemistry - A European Journal, 2017, 23, 2461-2468, which has been published in final form at: https://doi.org/10.1002/chem.201605547

All rights reserved.